Available online at www.sciencedirect.com
ScienceDirect
Polymer 47 (2006) 7374–7381
polymer
www.elsevier.com/locate/polymer

Poly(L-lactide) comb polymer brushes on the surface of clay layers

Yongfang Yang [a], Dongxia Wu [a], Chenxi Li [b], Li Liu [b], Xiaohui Cheng [a], Hanying Zhao [a,*]

[a] *Key Laboratory of Functional Polymer Materials, Ministry of Education, Department of Chemistry, Nankai University, Weijin Road, Tianjin 300071, PR China*
[b] *Institute of Polymer Chemistry, Nankai University, Weijin Road, Tianjin 300071, PR China*

Received 31 March 2006; received in revised form 7 July 2006; accepted 17 August 2006
Available online 11 September 2006

Abstract

Poly(L-lactide) (PLLA) comb polymers on poly(hydroxyethyl methacrylate) (PHEMA) backbone were prepared on the surface of clay layers by a combination of in situ atom transfer radical polymerization (ATRP) and ring-opening polymerization. An ATRP initiator with a quaternary ammonium salt end group was intercalated into the interlayer spacing of clay. PHEMA polymer brushes on the surface of clay layers were prepared by in situ ATRP. PLLA comb polymers on PHEMA backbone were prepared by ring-opening polymerization. X-ray diffraction (XRD) and transmission electron microscopy (TEM) results showed that with the increase of comb chain length more and more exfoliated structure was created. Aggregation of wormlike comb polymer brushes on the surface of clay layers was observed by TEM. Differential scanning calorimeter (DSC) results indicated that both the melting points and glass transition temperatures of the comb polymer brushes increase with the increase of comb chain length. The equilibrium melting temperature of the comb polymer brush on the surface of clay layers is lower than cleaved polymer. An atomic force microscopy (AFM) image proves the formation of wormlike structure by cleaved comb polymers.
© 2006 Published by Elsevier Ltd.

Keywords: Clay; Comb polymer brushes; Nanocomposites

1. Introduction

Over the past decade, much research has been focused on polymer/clay nanocomposites [1–3]. Nanocomposites in which clay is well-dispersed at relatively low loadings generally exhibit significant improvement in many properties, such as mechanical properties [4,5], thermal stability [6], and flame retardance [7,8]. Several methods have been used in the preparation of exfoliated clay–polymer nanocomposites, e.g., in situ polymerization of monomers [9–28], melt blending [29,30], and solution blending in polar solvents [31–33]. Of all the methods used in the preparation of nanocomposites, in situ polymerization method offers the best control over the polymer architecture and the structure of the composites.

Various different polymerization technologies were employed in the preparation of clay–polymer nanocomposites by in situ polymerization method. Surfactants with double bonds or free-radical initiator groups were tethered to the clay particles and polymer/clay nanocomposites were synthesized by free-radical polymerization [9–12]. Exfoliated poly(ε-caprolactone), and epoxy/clay nanocomposites were successfully synthesized via ring-opening polymerization [13–16]. Polyolefine–clay nanocomposites were prepared by using palladium or metallocene/clay catalysts [17–19]. From a surface-bound 1,1-diphenylethylene initiator, PS/clay composites were synthesized by living anionic polymerization [20,21]. Because living radical polymerization (LRP) methods allow better control over the molecular weight and distribution of the target polymer, a variety of LRP methods were used in the production of well-dispersed silicate layers, including ATRP method [22–25], nitroxide-mediated polymerization (NMP) method [26] and reversible addition–fragmentation chain transfer (RAFT) polymerization method [27,28]. Recently

* Corresponding author. Tel.: +86 22 2350 3930.
E-mail address: hyzhao@nankai.edu.cn (H. Zhao).

0032-3861/$ - see front matter © 2006 Published by Elsevier Ltd.
doi:10.1016/j.polymer.2006.08.053

Zhao and Shipp have proved that ATRP is successful in the synthesis of nanocomposites of layered silicate and well-defined block copolymers [23,24], and study of nanopatterns created by block copolymer chains on the surface of silicate layers is also possible [25].

In these years more and more people are interested in the study of biodegradable polymers with excellent properties. Polylactide (PLA) is of significant interest in medical applications such as wound closure, tissue culture and controlled release systems etc. [34]. Nanocomposites of clay and PLA will find great applications in medical science field. Preparation of clay/PLA nanocomposites by using solution blending method was reported before [33].

Synthesis of comb polymers has attracted much interest due to their specific conformation. The comb polymers with densely grafted side chains can adopt a wormlike cylinder brush conformation in a good solvent. In a recent publication, we reported the preparation of poly(DL-lactide)–poly(butyl acrylate) (PLA–PBA) comb-coil polymer brushes on the surface of silica nanoparticles [35]. In this paper for the first time we report the preparation and characterization of poly(L-lactide) (PLLA) comb polymer brushes on the surface of silicate layers by using a combination of in situ ATRP and in situ ring-opening polymerization (Scheme 1). An ATRP initiator with a quaternary ammonium salt end group (designated as R) was intercalated into the interlayer spacing of clay layers via ion-exchange. Subsequent in situ ATRP of hydroxyethyl methacrylate (HEMA) in the presence of CuBr and bipyridine afforded PHEMA backbone. PLLA comb polymers were grown from PHEMA backbone by ring-opening polymerization. Due to special conformation of comb polymers on the surface of clay layers, this type of polymers is supposed to have strong capability to create exfoliated structure in the nanocomposites.

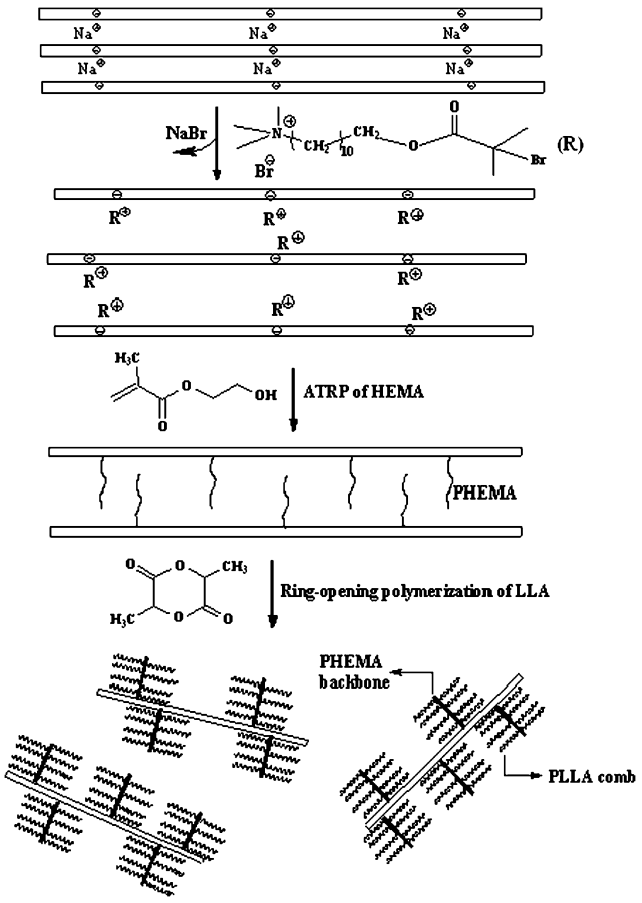

Scheme 1. Schematic representation for the preparation of PLLA comb polymer brushes on the surface of clay layers.

2. Experimental section

2.1. Materials

Sodium-montmorillonite with an ion-exchange capacity of 80 mequiv/100 g was kindly provided by Süd-chemie company under a commercial name of EX M 757. L-Lactide purchased from Tian-yuan Biomaterials Company was purified by recrystallization from ethyl acetate and dried in vacuum at room temperature. 2-Hydroxyethyl methacrylate (HEMA) was purchased from Tian Jin Institute of Chemical Agents, before use it was distilled at a reduced pressure. 2,2′-Dipyridine (bpy) and CuBr were purchased from Guo Yao Chemical Company. Before use dipyridine was recrystallized from hexane and dried in vacuum. CuBr was purified by washing with glacial acetic acid. Tin(II) 2-ethylhexanoaten was purchased from Aldrich, and was used as received. 11-Bromo-1-undecanol (Aldrich), 2-bromo-2-methyl propionyl bromide (Aldrich) and trimethyl amine (Aldrich) were used as received.

2.2. Preparation of ATRP initiator 11′-(*N*,*N*,*N*-trimethylammonium bromide)-undecyl-2-bromo-2-methyl propionate

ATRP initiator 11′-(*N*,*N*,*N*-trimethylammonium bromide)-undecyl-2-bromo-2-methyl propionate was synthesized using a procedure similar to the literatures [22,24]. 11′-Bromo-undecyl-2-bromo-2-methyl propionate was obtained by adding 2-bromo-2-methyl propionyl bromide/diethyl ether solution into 11-bromo-1-undecanol/pyridine/diethyl ether solution. After filtration the reaction mixture was reduced and washed with distilled water. The ester was further purified with silica column chromatography (a mixture of petro ether and ethyl acetate with a volume ratio of 20:1). The yield is about 80.5%. 11′-(*N*,*N*,*N*-Trimethylammonium bromide)-undecyl-2-bromo-2-methyl propionate was prepared by a reaction of 11′-bromo-undecyl-2-bromo-2-methyl propionate with trimethyl amine in ethanol. After removal of ethanol, the product was precipitated and washed with cold ether. Isolated yield is about 85.1%. ^{1}H NMR (300 MHz, dimethyl sulfoxide-d_6): 1.28 (m, 14H, $(CH_2)_7$), 1.55–1.74 (m, 4H, $2CH_2$), 1.88 (s, 6H, $(CH_3)_2$), 3.03 (s, 9H, $N(CH_3)_3$), 3.21–3.32 (m, 2H, CH_2N), 4.12 (t, 2H, CH_2O).

2.3. Preparation of the ATRP-initiator/clay composites

The ATRP initiator 11′-(*N*,*N*,*N*-trimethylammonium bromide)-undecyl-2-bromo-2-methyl propionate was ion-exchanged

onto clay layers. ATRP initiator (1.09 g) was dissolved in 100 ml distilled water, and then it was added to a solution of 2.5 g of clay in 1000 ml distilled water. The mixture was stirred for 30 h, after which the solids were filtered, washed, and dried in a vacuum oven at room temperature.

2.4. Preparation of the polymer/clay composites

2.4.1. Preparation of PHEMA/clay nanocomposites

In nitrogen atmosphere 22.95 mg CuBr, 75 mg bpy and 0.97 ml HEMA monomer were added into 3 ml isopropanol in a Schlenk flask. After CuBr was dissolved totally, the solution was transferred to another Schlenk flask with 0.2 g of ATRP-initiator/clay composites. The flask was purged by vacuum and then flushed with nitrogen. The mixture was stirred at room temperature for 18 h. After polymerization the nanocomposite was dispersed in methanol solution and precipitated in a mixture of toluene and THF (1/1, by volume). After filtration the solids were dried in a vacuum at 40 °C for one week.

2.4.2. Preparation of PLLA comb polymer/clay nanocomposites

In nitrogen atmosphere 4 ml DMF was added into a Schlenk flask with 0.1 g of PHEMA/clay nanocomposites. After the solids were dispersed well in the solution, varying amounts of LLA monomer were added. All the LLA monomer was dissolved in the solution when the temperature was increased to 100 °C. After tin(II) 2-ethylhexanoaten was added to the above solution, the reaction was stirred at 100 °C for 41 h. The PLLA comb chain length was controlled by the amount of monomer and tin(II) 2-ethylhexanoaten catalyst added into the reaction.

PHEMA and PLLA comb polymers were cleaved from clay by refluxing of the nanocomposites in methanol (for PHEMA) or THF/methanol (for PLLA comb polymers, 80/20 v/v) solutions of LiBr for 3 h, followed by centrifugation and filtration to remove clay layers from the solutions.

2.5. Characterization

The thermal properties of the nanocomposites were measured by thermogravimetric analysis (TGA). The samples were heated to 900 °C at a heating rate of 10 K/min under nitrogen atmosphere on a Netzsch TG 209. Differential scanning calorimeter (DSC) measurements were run on a Netzsch DSC 204. ^{1}H NMR spectra were recorded on a Varian 300 spectrometer. ATRP initiator and PHEMA were measured in deuterated DMSO and PLLA comb polymers were measured in deuterated chloroform. Transmission electron microscopy (TEM) observations were made on a JEM-100CX II operated at 100 kV. X-ray diffraction (XRD) study was carried out on a D/max-2500 diffractometer with Cu Kα radiation ($\lambda = 1.5406$ Å). Atomic force microscopy (AFM) images were collected on a Nanoscope IV atomic force microscope (Digital Instruments Inc.). The microscope was operated in tapping mode using Si cantilevers with a resonance frequency of 320 kHz. The voltage was between 2 and 3 V, and a tip radius was less than 10 nm. A drive amplitude of 1.2 V and a scan rate of 1.0 Hz were used.

3. Results and discussion

Two polymerization steps were involved in the synthesis of PLLA comb polymer brushes on the surface of clay layers. The process is illustrated in Scheme 1. At the first step, PHEMA brushes on the surface of ATRP-initiator anchored clay layers were prepared by using ATRP. At the second step, PLLA comb polymer brushes were synthesized on the backbone of PHEMA by using ring-opening polymerization. In order to synthesize PHEMA polymer brushes, an ammonium initiator used for ATRP was synthesized and then intercalated onto clay layers by ion-exchange.

TGA of the original clay (curve a in Fig. 1) was found to have 9% weight loss in the range between 100 and 800 °C. Upon addition of ATRP initiator, the composite was found to have 35% weight loss, so 26 wt% of the composite was alkyl ammonium initiator, which corresponds to approximately 97% of the Na^+ ions having been exchanged for the ATRP initiator. TGA result of PHEMA/clay (curve c) shows a 70% weight loss in the range between 280 and 430 °C, and a total of 12 wt% remained at 800 °C. For a comb polymer/clay nanocomposite (curve d) TGA result shows that a 93% weight loss in the range between 280 and 430 °C, and only 2 wt% remained at 800 °C.

XRD results (Fig. 2) prove that ATRP initiator was intercalated onto the surface of clay layers. In Fig. 2 curves a and b represent XRD spectra of original clay and ATRP-initiator modified clay, respectively. The XRD results indicate that the d_{001} spacing increased from 0.98 nm for the original clay to 1.84 nm for the ATRP-initiator intercalated clay.

ATRP of HEMA was initiated by alkyl ammonium initiator on the surface of clay layers. ^{1}H NMR spectrum of PHEMA is shown as spectrum A in Fig. 3. Cleaved PHEMA from the

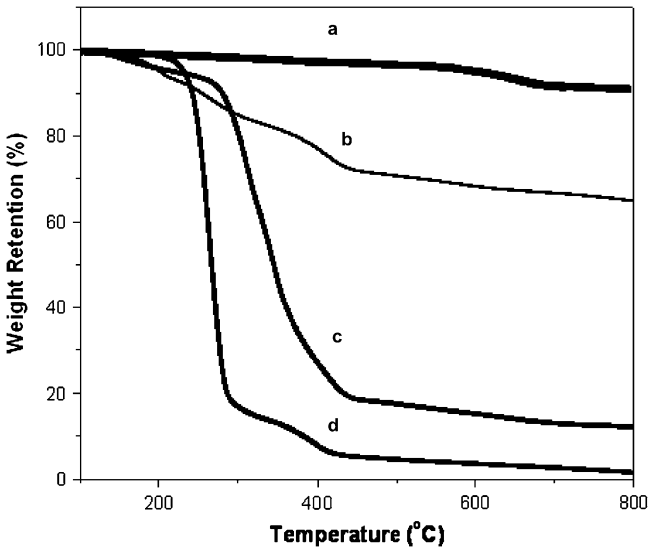

Fig. 1. TGA curves of unmodified clay (a), ATRP-initiator modified clay (b), PHEMA/clay nanocomposite (c) and $PLLA_{10}$–PHEMA/clay nanocomposite (d).

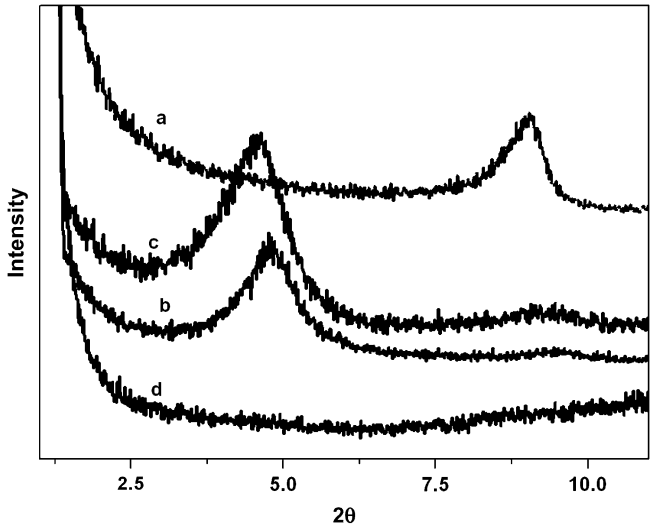

Fig. 2. X-ray diffraction curves of original clay (a), ATRP-initiator modified clay (b), PHEMA/clay nanocomposite (c), and $PLLA_{120}$–PHEMA/clay nanocomposites (d).

surface of clay layers was used in the ^{1}H NMR measurement. In Fig. 3 the peaks at 3.6 ppm (d) and 3.9 ppm (c) are assigned to methylene protons of ester group adjacent to the –OH group and –COO– group, respectively. The peak at 4.8 ppm (e) is assigned to the proton on –OH group. The peak at 3.03 ppm (indicated by an arrow on the spectrum) represents nine methyl protons of ammonium group at the end of PHEMA chain. A magnified peak at 3.03 ppm is also shown in Fig. 3. Using the ratio of peak area at 3.03 ppm to that at 3.6 ppm, the average number of PHEMA repeating units can be obtained. The calculation result shows that the average number of PHEMA repeating units is about 58. The XRD spectrum of PHEMA/clay is shown in Fig. 2. The diffraction peak at $2\theta = 4.8^\circ$ ($d_{001} = 1.95$ nm) can be observed, indicating that due to the low molecular weight of PHEMA, most of the clay layers still keep intercalated structure after in situ ATRP of HEMA.

PLLA comb polymers were prepared on the backbone of PHEMA by using ring-opening polymerization. Fig. 3 shows ^{1}H NMR spectrum of a cleaved comb polymer (spectrum B). On the spectrum the peaks at 4.8 and 3.6 ppm assigned to the proton on the –OH group and methylene protons adjacent to the –OH group in PHEMA disappear, which indicates the successful ring-opening reaction of LLA by –OH group on PHEMA backbone. On the spectrum the peaks at 4.35 (h) and 5.16 (i) ppm represent the methylene protons of ester group on PHEMA backbone and the methine protons on the PLLA comb chain. Using these two peaks, the molar ratio of PHEMA repeating units to PLLA repeating units can be obtained. Because the number of PHEMA repeating units is 58, the average number of PLLA repeating units on a comb chain can be calculated. Our calculation results show that the average numbers are 10, 92 and 120. In this paper all PLLA comb polymers with different chain lengths were synthesized on the PHEMA backbone with same molecular weight. The comb polymer/clay nanocomposites used in this paper are designated as $PLLA_{120}$–PHEMA/clay, $PLLA_{92}$–PHEMA/clay and $PLLA_{10}$–PHEMA/clay, respectively. GPC results indicate that the polydispersities of the polymer brushes are 1.26 for $PLLA_{10}$–PHEMA, 1.49 for $PLLA_{92}$–PHEMA and

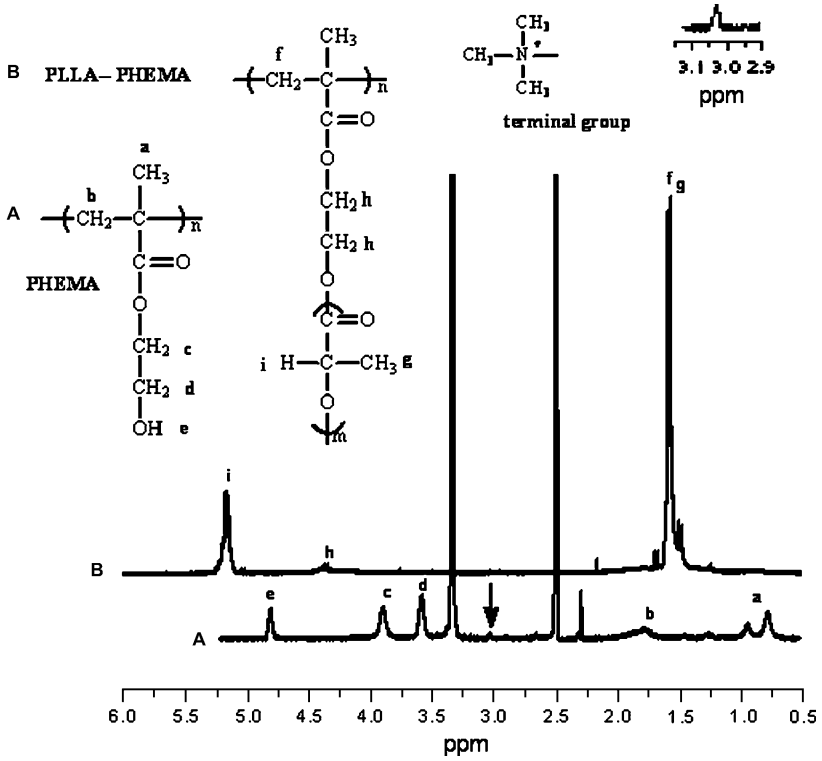

Fig. 3. ^{1}H NMR spectra of cleaved PHEMA (spectrum A) and $PLLA_{10}$–PHEMA comb polymer (spectrum B).

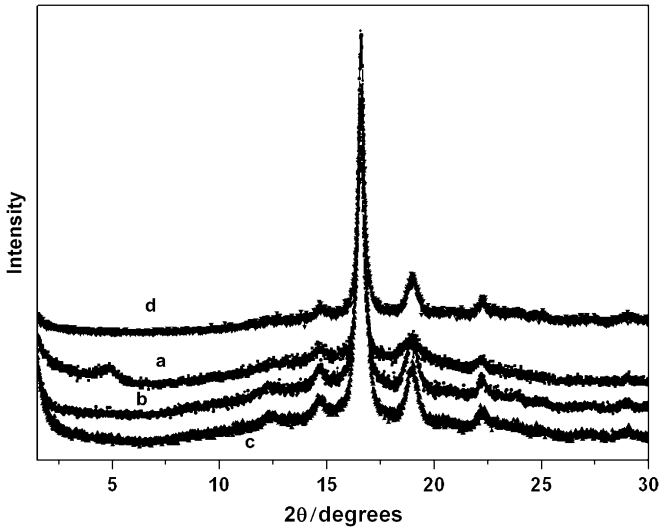

Fig. 4. X-ray diffraction curves of nanocomposites of (a) $PLLA_{10}$–PHEMA/clay, (b) $PLLA_{92}$–PHEMA/clay, (c) $PLLA_{120}$–PHEMA/clay, and (d) neat $PLLA_{120}$ comb polymer cleaved from clay layers.

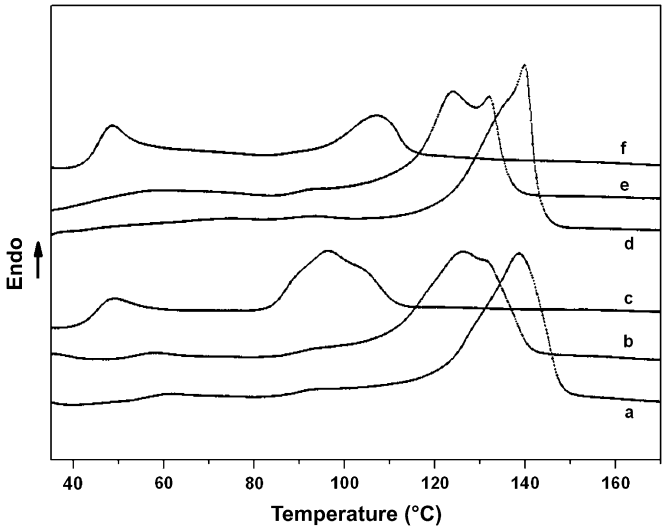

Fig. 5. DSC traces of (a) $PLLA_{120}$–PHEMA/clay, (b) $PLLA_{92}$–PHEMA/clay, (c) $PLLA_{10}$–PHEMA/clay, and (d) cleaved $PLLA_{120}$–PHEMA, (e) cleaved $PLLA_{92}$–PHEMA and (f) cleaved $PLLA_{10}$–PHEMA.

1.57 for $PLLA_{120}$–PHEMA, which means that the polydispersity index increases with the increase of comb chain length.

Fig. 4 shows WAXD profiles of one neat PLLA comb polymer and three PLLA–PHEMA/clay nanocomposites. For $PLLA_{10}$–PHEMA/clay nanocomposite there is a broad peak at around $2\theta = 4.7°$ indicating that the well-ordered intercalated structure in the nanocomposites was not destroyed totally. However, for the other two nanocomposites, no peak can be found in the range between $2\theta = 2°$ and 10°, which means that in the nanocomposites with increase of the PLLA comb chain length more and more intercalated structures were destroyed and clay layers randomly dispersed in polymer matrix, and finally exfoliated structure predominates. The absence of XRD signals at low angles does not provide definitive proof of complete exfoliation because the silicate was diluted by polymer. Furthermore, XRD is not quantitative in determining the amount of exfoliation versus intercalation [36]. PLLA is a kind of crystalline polymer, WAXD can be employed as a powerful tool in the study of crystal structure of PLLA. In Fig. 4 all samples exhibit very strong peaks at $2\theta = 16.6°$ due to diffraction from (200) plane accompanied by two diffraction peaks at $2\theta = 19.5°$ and 15.3°. The peaks at $2\theta = 19.5°$ and 15.3° are due to diffraction from (203) plane and (010) plane, respectively [37]. These profiles indicate that neat PLLA comb chains or PLLA comb chains on the surface of clay layers form orthorhombic crystal [37,38]. Nam et al. studied crystallization behavior of PLLA/layered silicate nanocomposites [37], they found that the neat linear PLLA has a strong (200) diffraction peak at $2\theta = 17.1°$; however, after it is intercalated into clay layers, the peak shifts to the lower angle. In our system the (200) diffraction angle of the neat PLLA comb polymer is lower than that of the neat linear PLLA, this is probably due to the conformation of the polymer chains. The comb structure limits the movement of polymer segments to the growth front, so comparing with linear PLLA crystal, there are more defects in the comb polymer crystals.

Fig. 5 represents DSC curves of cleaved comb polymers and comb polymer/clay nanocomposites. For PLLA–PHEMA/clay nanocomposites, the melting points of PLLA comb decrease with the decrease in comb chain length. The melting temperature of PLLA comb in $PLLA_{120}$–PHEMA/clay is at about 138.5 °C, however, for $PLLA_{92}$–PHEMA/clay and $PLLA_{10}$–PHEMA/clay the melting point shifts to 125.9 and 96.3 °C, respectively. Accompanying the decrease of the melting points, the melting peaks get broader. For cleaved comb polymers, similar phenomenon can also be found. The DSC results indicate that there are more defects in the crystals of comb polymer with shorter comb chains. For nanocomposites the glass transition temperatures (T_g's) of PLLA comb polymer brushes also decrease with the decrease of comb chain length. For $PLLA_{120}$–PHEMA/clay, T_g of PLLA is at about 55 °C, however, with the decrease of comb chain length T_g shifts to 52 °C for $PLLA_{92}$–PHEMA/clay and 48 °C for $PLLA_{10}$–PHEMA/clay. Similar trend can also be found for cleaved comb polymers.

Fig. 6 shows that the melting temperatures of neat $PLLA_{120}$–PHEMA comb polymer and its nanocomposite increase by increasing the isothermal crystallization temperature (T_c), indicating that the perfection and thickness of the growing PLLA lamella crystals increase at higher crystallization temperatures. By fitting these data points to a straight line and extrapolating it to $T_m = T_c$, the equilibrium melting temperature, T_m^o, can be obtained. The T_m^o values for cleaved $PLLA_{120}$–PHEMA comb polymer and its nanocomposite are 425.7 K and 422.5 K, respectively. The T_m^o value for cleaved PLLA comb is lower than Krikorian's value of 471 K [39a], Vasanthakumari's value of 480 K [39b], or Kalb's value of 488 K all for linear PLLA polymer [39c]. This might be due to the differences in the conformation of the samples used in the experiments. For $PLLA_{120}$–PHEMA comb polymer stretched PLLA comb chains densely distribute on the PHEMA backbone. Comparing with linear PLLA this structure is unfavorable for

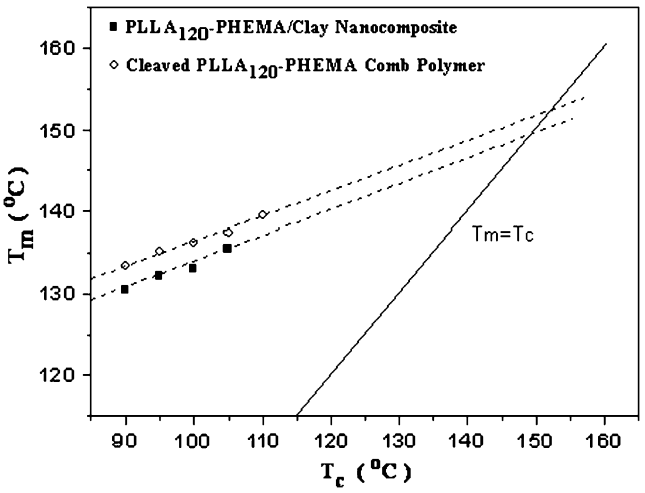

Fig. 6. Crystallinity melting point, T_m, as a function of the crystallization temperature, obtained from DSC measurements. The extrapolation of the lines fitted to the experimental data at $T_m = T_c$ are shown as dashed lines.

the crystallization of PLLA, so the thickness of the lamella in PLLA crystal is thinner and there are more defects in the crystals. In Fig. 6 it can be observed that the equilibrium melting point in the case of nanocomposite is lower than cleaved comb polymer, suggesting the existence of thinner lamella crystals or defective crystalline regions in the nanocomposite.

TEM images of the PLLA–PHEMA/clay nanocomposites are presented in Fig. 7. These images indicate that with the growth of comb chain length a significant degree of silicate exfoliation was achieved. Fig. 7a is a TEM image of $PLLA_{10}$–PHEMA/clay at a low magnification. This image shows large clay particles and their aggregation. In the nanocomposite the comb chain is very short (10 LLA repeating units), significant dispersion has not been achieved. Fig. 7b is a TEM image of $PLLA_{92}$–PHEMA/clay at a low magnification. On the image most of the big clay particles disappear. Fig. 7c is a TEM image of $PLLA_{92}$–PHEMA/clay at a high magnification. Although intercalated structure is present in the image, exfoliated clay layers in polymer matrix can be observed.

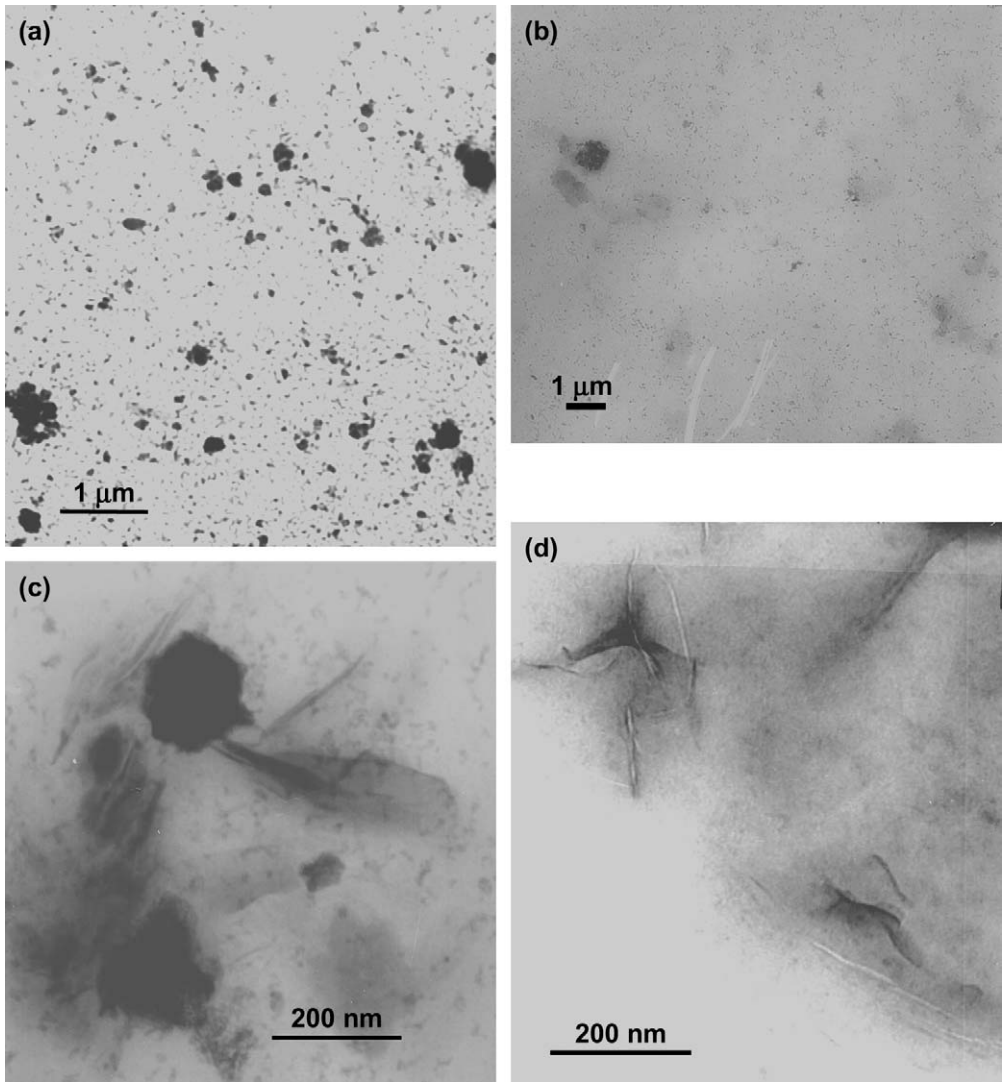

Fig. 7. TEM images of (a) $PLLA_{10}$–PHEMA/clay at a low magnification, (b) $PLLA_{92}$–PHEMA/clay at a low magnification, (c) $PLLA_{92}$–PHEMA/clay at a high magnification, and (d) $PLLA_{120}$–PHEMA/clay at a high magnification.

Fig. 7d is a TEM image of $PLLA_{120}$–PHEMA/clay. On the image it appears that this nanocomposite achieved great exfoliation than previous two samples. The TEM results suggest that with the increase of comb chain length, more and more intercalated structure was destroyed and exfoliated structure was created, which is consistent with previous XRD results.

In order to observe comb polymer brushes on the surface of clay layers, $PLLA_{120}$–PHEMA/clay nanocomposite was dispersed in $CHCl_3$ solution and a dipped specimen was observed on a TEM image after being stained by hydrazine hydrate and OsO_4. The reason why this sample was chosen for TEM measurement is that in this nanocomposite there are most exfoliated clay layers, and polymer brushes only on the surface of exfoliated clay layers can be observed clearly on a TEM image [23,25]. A TEM image of comb polymer brushes on the surface of an exfoliated clay layer is shown in Fig. 8. The inset in Fig. 8 is a magnification of a part of isolated clay layer. On the image the polymer brushes can be observed clearly. The tethered comb polymer brushes tend to aggregate together on the clay surface. Because of the high density of polymer brushes on the surface, it is hard to measure the size of an isolated comb polymer molecule.

Due to the densely grafted side chains the comb polymers adopt a wormlike cylinder brush conformation, in which the side chains are stretched in the direction of the backbone. AFM is frequently used in the study of comb polymers [40–42]. In this work AFM was also employed to observe neat comb molecules cleaved from clay layers. The cleaved $PLLA_{120}$–PHEMA comb polymer was deposited from a dilute solution on the surface of a freshly cleaved mica. To visualize single molecules a highly diluted solution ($c = 0.01$ g/L) of comb polymer in $CHCl_3$ was sprayed onto mica (Fig. 9). On the image wormlike cylinders are clearly visible. A statistical analysis of the image shows that the length of the cylinders ranges from 20 to 50 nm and the width ranges from 8 to 12 nm. Thus, AFM result proves once more that the well-defined comb polymer brushes were synthesized on the surface of clay layers.

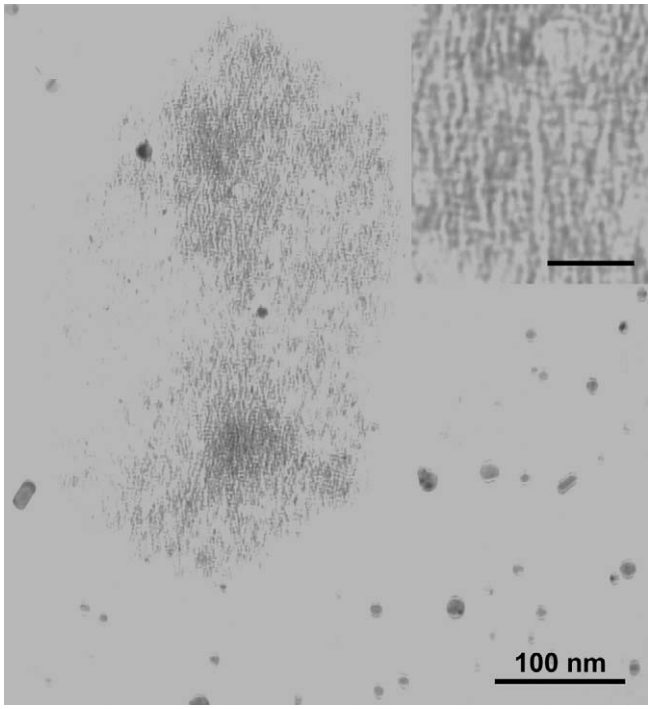

Fig. 8. A TEM image of $PLLA_{120}$–PHEMA/clay nanocomposite dispersed in $CHCl_3$ solution. The specimen was prepared by dipping a copper grid in the solution and by drying in air. In order to increase the contrast, the specimen was stained by hydrazine hydrate and OsO_4, respectively. The inset is a magnification of a part of isolated clay layer with block copolymer brushes and the scale bar represents 50 nm.

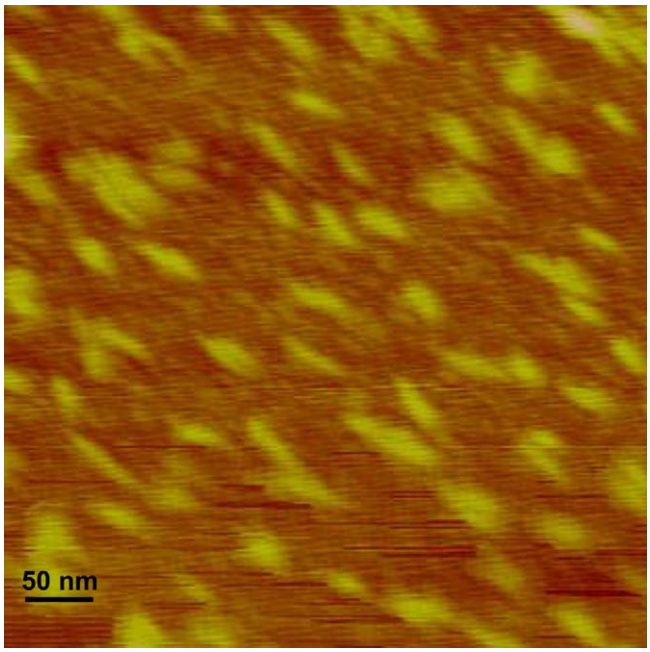

Fig. 9. A tapping mode AFM image of cleaved $PLLA_{120}$–PHEMA comb polymer. The sample was prepared on a freshly cleaved mica.

4. Conclusions

PLLA comb polymers on PHEMA backbone were successfully prepared on the surface of clay layers. The structure of the nanocomposites depends on the length of PLLA chain. With the increase of the PLLA chain length, more exfoliated structure is created in the nanocomposites. PLLA comb chains on the surface of clay layers form orthorhombic crystal. The equilibrium melting temperature of the comb polymer brush is lower than cleaved comb polymer and linear polymer reported in the literatures. Comb polymer brushes on the clay layers were observed by TEM. An AFM image shows wormlike structure of cleaved comb chains.

Acknowledgment

This project was supported by National Natural Science Foundation of China under contract nos. 20544001 and 20574037, and start-up funds from Nankai University.

References

[1] Alexandre M, Dubois P. Mater Sci Eng 2000;28:1.
[2] Zanetti M, Lomakin S, Camino G. Macromol Mater Eng 2000;279:1.
[3] Pinnavaia TJ, Beall GW. Polymer–clay nanocomposites. New York: Wiley; 2000.
[4] Lan T, Pinnavaia TJ. Chem Mater 1994;6:2216.
[5] Wang Z, Pinnavaia TJ. Chem Mater 1998;10:1820.
[6] Messersmith P, Giannelis EP. Chem Mater 1994;6:1719.
[7] Jang BN, Costache M, Wilkie CA. Polymer 2005;46:10678.
[8] Zhu J, Uhl FM, Morgan AB, Wilkie CA. Chem Mater 2001;13:4649.
[9] Zhu J, Morgan AB, Lamelas FJ, Wilkie CA. Chem Mater 2001;13:3774.
[10] Zeng C, Lee LJ. Macromolecules 2001;34:4098.
[11] Fu X, Qutubuddin S. Polymer 2001;42:807.
[12] Fan X, Xia C, Fulghum T, Park M, Locklin J, Advincula RC. Langmuir 2003;19:916.
[13] Messersmith PB, Giannelis EP. J Polym Sci Polym Chem Ed 1995;33:1047.
[14] Kubies D, Pantoustier N, Dubois P, Rulmont A, Jerome R. Macromolecules 2002;35:3318.
[15] Lan T, Kaviratna PD, Pinnavaia TJ. Chem Mater 1995;7:2144.
[16] Brown JM, Culiss D, Vaia RA. Chem Mater 2000;12:3376.
[17] Bergman JS, Chen H, Giannelis EP, Thomas MG, Coates GW. Chem Commun 1999;21:2179.
[18] Tudor J, Willington L, O'Hare D, Royan B. Chem Commun 1996;17:2031.
[19] (a) Sun T, JGarcés JM. Adv Mater 2002;14:128;
(b) He A, Wang L, Li J, Dong J, Han CC. Polymer 2006;6:1767.
[20] Fan X, Zhou Q, Xia C, Cristofoli W, Mays J, Advincula R. Langmuir 2002;18:4511.
[21] Zhou Q, Fan X, Xia C, Mays J, Advincula R. Chem Mater 2001;13:2465.
[22] Böttcher H, Hallensleben ML, Nuss S, Wurm H, Bauer J, Behrens P. J Mater Chem 2002;12:1351.
[23] Zhao H, Shipp DA. Chem Mater 2003;15:2693.
[24] Zhao H, Argoti SD, Farrell BP, Shipp DA. J Polym Sci Polym Chem Ed 2004;42:916.
[25] Zhao H, Farrell BP, Shipp DA. Polymer 2004;45:4473.
[26] Weimer MW, Chen H, Giannelis EP, Sogah DY. J Am Chem Soc 1999;121:1615.
[27] Zhang B, Pan C, Hong C, Luan B, Shi P. Macromol Rapid Commun 2006;27:97.
[28] Salem N, Shipp DA. Polymer 2005;46:8573.
[29] Burnside SD, Giannelis EP. Chem Mater 1995;7:1597.
[30] Maiti P, Nam PH, Okamoto M, Hasegawa N, Usuki A. Macromolecules 2002;35:2042.
[31] Zha W, Choi S, Lee KM, Han CD. Macromolecules 2005;38:8418.
[32] Tien YI, Wei KH. Macromolecules 2001;34:9045.
[33] Krikorian V, Pochan DJ. Chem Mater 2003;15:4317.
[34] Kubo H, Sato H, Okamoto M, Kotaka T. Polymer 1998;39:501.
[35] Zhao H, Kang X, Liu L. Macromolecules 2005;38:10619.
[36] Vaia RA, Liu W. J Polym Sci Part B Polym Phys 2002;40:1590.
[37] Nam JY, Ray SS, Okamoto M. Macromolecules 2003;36:7126.
[38] Hoogsteen W, Postema AR, Pennings AJ, Brinke GT, Zugenmaier P. Macromolecules 1990;23:634.
[39] (a) Krikorian V, Pochan DJ. Macromolecules 2004;37:6480;
(b) Vasanthakumari R, Pennings AJ. Polymer 1983;24:175;
(c) Kalb B, Pennings AJ. Polymer 1980;21:607.
[40] Dziezok P, Sheiko SS, Fischer K, Schmidt M. Angew Chem Int Ed Engl 1997;36:2812.
[41] Sheiko SS, Prokhorova SA, Beers KL, Matyjaszewski K, Potemkin II, Khokhlov AR, et al. Macromolecules 2001;34:8354.
[42] Lord SJ, Sheiko SS, Larue I, Lee H, Matyjaszewski K. Macromolecules 2004;37:4235.